JOC The Journal of Organic Chemistry

Article

pubs.acs.org/joc

Synthesis of Carba-NAD and the Structures of Its Ternary Complexes with SIRT3 and SIRT5

Bruce G. Szczepankiewicz,*[,†] Han Dai,[†] Karsten J. Koppetsch,[†] Dongming Qian,[‡] Fan Jiang,[‡] Cheney Mao,[‡] and Robert B. Perni[†]

[†]Sirtris, a GSK Company, 200 Technology Square, Cambridge, Massachusetts 02139, United States

[‡]Viva Biotech Ltd., 334 Aidisheng Road, Zhangjiang High-tech Park, Shanghai 201203, China

Supporting Information

ABSTRACT: Carba-NAD is a synthetic compound identical to NAD except for one substitution, where an oxygen atom adjacent to the anomeric linkage bearing nicotinamide is replaced with a methylene group. Because it is inert in nicotinamide displacement reactions, carba-NAD is an unreactive substrate analogue for NAD-consuming enzymes. SIRT3 and SIRT5 are NAD-consuming enzymes that are potential therapeutic targets for the treatment of metabolic diseases and cancers. We report an improved carba-NAD synthesis, including a pyrophosphate coupling method that proceeds in approximately 60% yield. We also disclose the X-ray crystal structures of the ternary complexes of SIRT3 and SIRT5 bound to a peptide substrate and carba-NAD. These X-ray crystal structures provide critical snapshots of the mechanism by which human sirtuins function as protein deacylation catalysts.

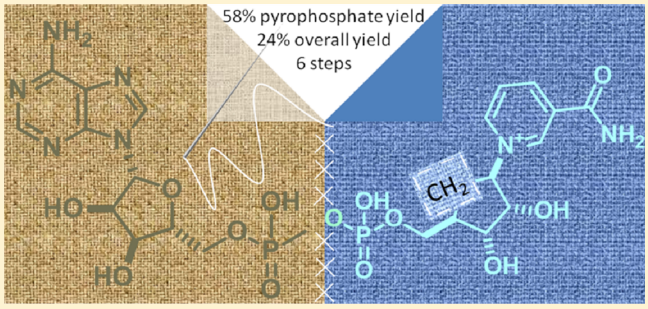

INTRODUCTION

In living organisms, nicotinamide adenine dinucleotide, or NAD (**1**), plays a central role in energy metabolism. The oxidation−reduction cycle between NAD (**1**) and NADH (**2**) is an ancient biochemical process, and it occurs in aerobic bacteria as well as in all higher organisms (Scheme 1). In the redox cycle, a hydride ion is captured and released by the niacinamide portion of NAD (**1**). Vitamin B_3 (niacinamide or nicotinamide) (**3**) is a human dietary nutrient because it is required for the biosynthesis of NAD (Scheme 2).

Scheme 1. The NAD−NADH Redox Pair

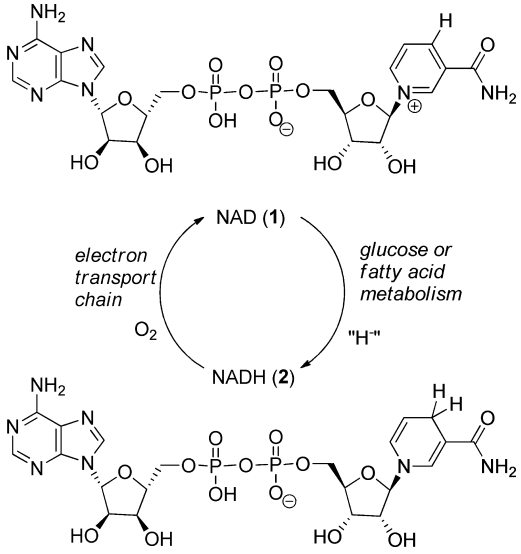

NAD also participates in reactions that displace nicotinamide (**3**) from the rest of the molecule. Simple hydrolysis of NAD generates a molecule of nicotinamide (**3**) and a molecule of adenosine diphosphoryl ribose, or ADPribose (**4**) (Scheme 2). This reaction is energetically favorable ($\Delta G \approx -8$ kcal/mol), and it is exploited in different biochemical processes.[1,2] The reaction between nucleophilic amino acid residues (Arg, Asn, Glu, Asp, Cys, Lys, modified His) and NAD can yield ADP-ribosylated proteins **5**. Mono-ADPribosyl transferases, or MARTs, catalyze this reaction in diverse organisms.[3] Poly-ADPribosylated proteins **6** are produced from proteins and NAD via a family of enzymes called poly-ADPribose polymerases or PARPs. PARP enzymes have been studied as targets for cancer chemotherapy.[4] Another family of enzymes known as cADPr synthases catalyze the formation of cyclic-ADPribose (**7**), which serves as an intracellular second messenger. The two most well-known cADPr synthases are CD38 and CD157. Both CD38 and CD157 are present on leukocytes and have been considered as targets for autoimmune diseases.[5] A fourth set of NAD-consuming enzymes are the sirtuins. These enzymes deacylate proteins and produce acyl-ADP-ribose esters such as **8** from NAD. The sirtuins are targets for many human diseases associated with aging, including diabetes, cancer, and neurodegenerative conditions.[6] Many different biochemical pathways are therefore dependent on

Received: May 23, 2012
Published: July 31, 2012

ACS Publications © 2012 American Chemical Society

dx.doi.org/10.1021/jo301067e | J. Org. Chem. 2012, 77, 7319−7329

Scheme 2. Role of NAD in Multiple Biochemical Processes Involving Nicotinamide Displacement

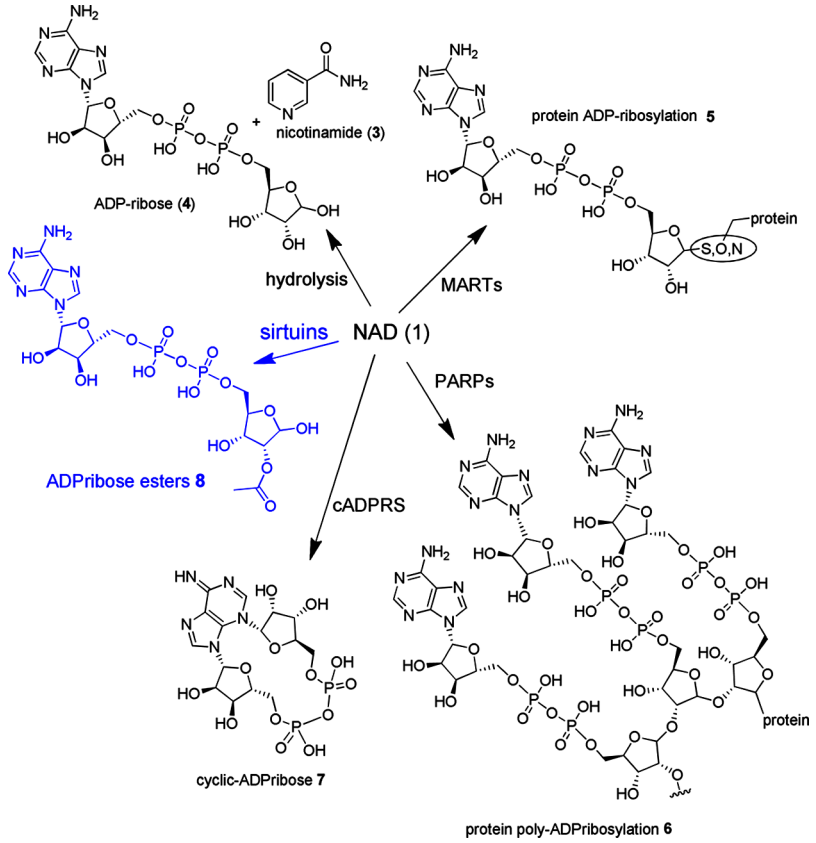

nicotinamide displacement from NAD, and several enzyme families participate directly in nicotinamide displacement reactions.

The putative role of NAD-consuming enzymes in human diseases has led to a great deal of work in studying their mechanisms of action.[3] X-ray crystal structures have been generated for several PARPs, cADPr synthases, and sirtuins. In addition to the native protein structures, X-ray crystal structures of the enzymes bound to NAD or a protein substrate have been solved.[5,7,8] These bound structures provide valuable information regarding the mechanism of catalysis. However, the most useful mechanistic information comes from complexes containing all of the reaction components. Binary complexes of cADPr synthases and NAD are short-lived. Similarly, ternary complexes of both NAD and a protein substrate bound to catalytically active PARPs or sirtuins are short-lived. In order to obtain an X-ray crystal structure of a reactive complex, it is necessary to stop the enzymatic reaction without disrupting ligand binding. This has been accomplished by using a catalytically inactive enzyme, modifying the substrate protein structure, cryogenically freezing the complex, or using an NAD analogue that does not undergo rapid nicotinamide displacement.[5,7−11]

Carba-NAD (**9**) is a synthetic analogue of NAD that was first described by Slama and Simmons in 1988.[12,13] Carba-NAD is identical to NAD except for one substitution, where an oxygen atom adjacent to the anomeric linkage bearing nicotinamide is replaced with a methylene group (Chart 1). This substitution renders carba-NAD inert in nicotinamide displacement reactions. It binds to many NAD-consuming enzymes in a manner very similar to NAD itself, but the reaction stops before nicotinamide displacement ensues. Therefore, carba-NAD can

Chart 1. Structure of Carba-NAD

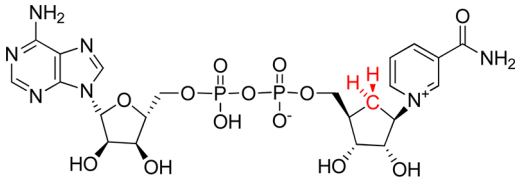

be used to probe the function of NAD-consuming enzymes.[14] Carba-NAD also participates in redox reactions in a manner similar to NAD.[12,15] Some enzyme kinetic work employing carba-NAD has been carried out in the past.[12−16] Additionally, two X-ray crystal structures of carba-NAD bound to the enzyme yHST2 have been published.[17,18] However, further work with carba-NAD has been hampered by its challenging synthesis. In a broader sense, NAD and NAD analogues are generally regarded as difficult compounds to prepare by chemical synthesis. NAD itself has been a target of organic synthesis for over 50 years, with steady improvements in yields and reproducibility as new reagents and more efficient purification strategies became available.[19−23] Perhaps the most challenging synthetic transformation has been the installation of the pyrophosphate linkage. Pyrophosphate coupling yields are notoriously capricious, and as the last step in many NAD syntheses, this transformation severely limits material throughput.[24] Because carba-NAD also contains a pyrophosphate linkage, a reliable pyrophosphate coupling method would overcome the most significant obstacle in its preparation. In turn, easier access to carba-NAD would increase its use in studying NAD-dependent biological processes.

dx.doi.org/10.1021/jo301067e | J. Org. Chem. 2012, 77, 7319−7329

Previously, we reported the X-ray crystal structure of human SIRT3. We also determined crystal structures of SIRT3 bound to three different ligands: (1) an acyl-peptide substrate, (2) the immediate product of the NAD-acyl peptide reaction, and (3) a deacylated peptide product.[25] However, the structure of the ternary complex of SIRT3/acyl-peptide/NAD could not be determined. The greatest challenge to obtaining such a structure is the short-lived nature of the ternary complex. The reaction between the acyl-peptide substrate and NAD occurs rapidly upon binding to SIRT3, precluding structural characterization.

To address this challenge, we used carba-NAD (**9**) which cannot react with the acyl-peptide substrate. In this article, we describe a six-step synthesis of carba-NAD that features no protecting groups. In the final step, we addressed the difficult pyrophosphate coupling by employing a nonaqueous buffering system that resulted in reliable and reproducible pyrophosphate bond formation. An ample supply of carba-NAD allowed us to solve a SIRT3/acyl-peptide/carba-NAD ternary complex crystal structure, providing a snapshot of the reactive complex for SIRT3-mediated protein deacetylation. We also report the crystal structure of a SIRT5/succinyl-peptide/carba-NAD ternary complex. This SIRT5 structure was compared to a recently published NAD-containing SIRT5 ternary complex, demonstrating that carba-NAD is an excellent NAD mimetic for crystallographic work.[26]

RESULTS

Synthesis of Carba-NAD. When we set out to prepare carba-NAD (**9**), the three key points we sought to address were to make the synthetic sequence as succinct as possible by eliminating protecting group manipulations, to find a reliable pyrophosphate coupling method, and to make the purification of carba-NAD as well as the water-soluble synthetic precursors easier. The first challenge was to prepare gram quantities of amino carba-ribose **10** (Scheme 3). Amine **10** is an intermediate for carbocyclic nucleoside synthesis and has been prepared in over 20 different published procedures.[12,13,27−46] The most attractive sequence was a three-step preparation starting from the commercially available *R*-(−)-Vince lactam **11**.[47,48] As reported by Cermak and Vince, dihydroxylation proceeds with good stereoselectivity, providing dihydroxy lactam **12** in 75% yield after removal of the undesired all-cis stereoisomer. Acid-catalyzed methanolysis of the lactam proceeded quantitatively, giving amino ester hydrochloride **13**.[12,44] Ester reduction was accomplished using lithium triethylborohydride.[12,38,41,42] Slightly more than 5 equiv of lithium triethylborohydride was used to ensure complete reduction of the ester to the alcohol. The first hydride equivalent was consumed as the amine HCl salt reacted to give the free base. An additional 2 equiv of hydride was then complexed with the amino diol. Finally, ester reduction proceeded rapidly at 0 °C upon addition of another 2 equiv of hydride. After the reaction was diluted with water, ^{1}H NMR analysis showed that all of the ester had been consumed, but the product resonances were shifted downfield from their expected positions.[37] Additionally, two resonances at approximately 0.0 ppm and 0.5 ppm were visible. These upfield resonances were characteristic of triethylborane complexed with the product, and the complex could not be disrupted by treatment with $HCl_{(aq)}$, $NaOH_{(aq)}$, or by chromatographic methods.[49] However, the boron complex could be broken instantly by the addition of $HF_{(aq)}$ at 0 °C. Two moles of HF per mole of lithium triethylborohydride was required to completely dissociate the product from triethylborane. Additional HF was added to ensure that the product precipitated as its HF salt. Although we did not rigorously characterize the boron-containing product produced by HF addition, the ^{1}H NMR spectrum clearly showed an ethyl borane resonance. On the basis of the 2: 1 stoichiometry of the HF addition, we propose that the byproduct is diethyldifluoroboric acid. After concentration of the aqueous solution, addition of acetonitrile precipitated the product **10** as its HF salt, while the boron-containing byproducts remained in solution. Treatment of the amine HF salt with LiOH provided amino carba-ribose **10** in its basic form. No chromatography was required to isolate **10**, which greatly facilitated the preparation of this key intermediate in multigram quantities.

Scheme 3. Synthesis of Carba-NAD (9) from *R*-(−)-Vince Lactam (11)[a]

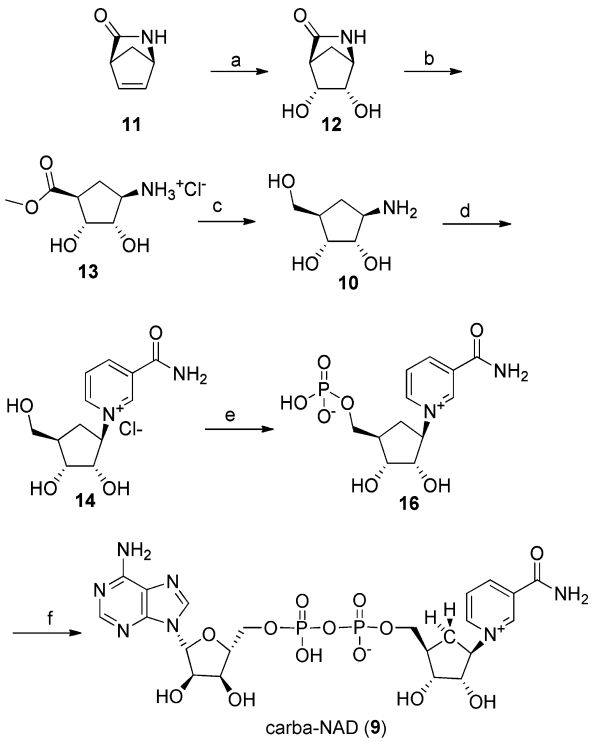

[a]Reagents and conditions: (a) OsO_4, NMO, H_2O, *tert*-pentyl alcohol, 70 °C (75%); (b) HCl, CH_3OH, 25 °C, (99%), (c) i. $LiEt_3BH$, THF, 0 °C, ii. $HF_{(aq)}$, 0 °C, iii. $LiOH_{(aq)}$ 25 °C (99%). (d) 3-carbamoyl-1-(2,4-dinitrophenyl)pyridin-1-ium chloride (**15**) NaOAc, CH_3OH, 25 °C (76%); (e) $POCl_3$, trimethyl phosphate, 0 °C, (76%); (f) $MnCl_2$, pyridine, *p*-TsOH, adenosine 5-monophosphomorpholidate 4-morpholine-*N*,*N*-dicylcohexylcarboxamidine salt, formamide (58%).

The next step was to prepare nicotinamide carba-riboside **14** from **10** and pyridinium salt **15**. Using a modification of the literature methods, we prepared and isolated pyridinium salt **15** as an amorphous yellow solid.[21] We found that the Zincke reaction proceeded quickly at ambient temperature in methanol solution, providing **14** in 75% yield.[50] Phosphorylation of **14** with $POCl_3$ according to Lee's procedure provided carba-nicotinamide mononucleotide **16** in 76% yield.[23] Purification was accomplished via chromatography over an aminopropyl-functionalized silica gel column. This allowed us to isolate **16** as its inner salt, setting the stage for the final pyrophosphate bond formation. Coupling of **16** with adenosine 5′-monophospho-

dx.doi.org/10.1021/jo301067e | J. Org. Chem. 2012, 77, 7319−7329

morpholidate, using pyridinium tosylate to buffer the reaction and $MnCl_2$ as a divalent cation source, allowed the desired pyrophosphate bond formation to proceed smoothly.[22] Importantly, the reaction gave a homogeneous solution in formamide, ensuring predictable mixing of the reagents. After the reaction was complete, major components of the crude reaction mixture included **9**, *N*,*N*′-dicyclohexylguanidine, pyridine, toluenesulfonic acid, $MnCl_2$, and adenosine-5′-monophosphate. Carba-NAD (**9**) was isolated from the other reaction components by eluting over an amine-functionalized silica gel column with methanolic and aqueous acetate buffers. Because methanol can be used as a mobile phase, a second pass of **9** over the column allowed for separation from sodium acetate. Subsequent elution with aqueous acetic acid followed by concentration of the product-containing fractions gave carba-NAD as its inner-salt in 58% isolated yield. The NMR spectral data were in agreement with those of Slama.[12] Carba-NAD displays solubility properties very similar to NAD. It is highly water-soluble, but insoluble in methanol, ethanol, DMSO, DMF, and less polar organic solvents. It was isolated as an amorphous white solid which can be stored dry at −20 °C for several months.

X-ray Crystal Structure of the SIRT3/ACS2 Peptide/Carba-NAD (9) Ternary Complex. The protein acetyl-Co-A synthase 2 (ACS2) is a known substrate for SIRT3. An *N*-ε-acetyl group on lysine 642 (K642) of the ACS2 protein is deacetylated by SIRT3 in mitochondria.[51] The peptide used in the cocrystallization experiments was a 12 amino acid fragment of ACS2 containing K642 (TRSG-Kac-V-Nle-RRLLR). The only difference between this peptide and the one reported previously is the substitution of norleucine for methionine to improve the peptide stability toward oxidation.[25]

Crystals of the SIRT3/ACS2/**9** ternary complex were obtained by soaking SIRT3/ACS2 crystals with a solution of 10 mM **9** in crystallization solution. Cracks in the crystals were observed upon soaking, which led to poor quality diffraction data. Therefore, the SIRT3/ACS2 crystals were stabilized by cross-linking with glutaraldehyde before soaking with carba-NAD (**9**). As a result, a 2.47 Å data set was collected for crystals of the SIRT3/ACS2/**9** ternary complex.

The overall fold of the SIRT3/ACS2/**9** ternary complex is very similar to the previously reported structure of the SIRT3/ACS2 complex (PDB code 3GLR), with a root-mean-square deviation (rmsd) of 0.7 Å for 272 Cα atoms.[25] The ACS2 peptide adopts an extended β-strand conformation, with the main chain amide groups forming hydrogen bonds with residues G295, E296, and residue E325 (Figure 1a). The methylene groups of the acetyl lysine side chain are located in a hydrophobic cavity lined by F294 and V324. The acetyl group is sandwiched between H248 and F180, with the *N*-ε amide proton forming a hydrogen bond to the carbonyl oxygen of V292. This hydrogen bond maintains the orientation and the extended conformation of the acetyl lysine side chain. The terminal methyl group of the acetyl lysine is in van der Waals contact with I291 and I230. Extra hydrophobic space is clearly available adjacent to the terminal methyl group, indicating that SIRT3 can accommodate *N*-ε-amides larger than acetate. This observation is consistent with the fact that SIRT3 also will remove an *N*-ε-propionyl amide from propionyl-lysine containing peptides. The carba-NAD shows well-defined electron density, with an average *B* factor of 73.96 $Å^2$, compared to the average *B* factor of 67.50 $Å^2$ for the protein atoms. Carba-NAD makes multipoint contacts with SIRT3: (1) the adenine ring makes hydrogen bonds with T150 and V366; (2) the amide group of the nicotinamide ring makes hydrogen bonds with I230 and D231 in the nicotinamide binding C pocket; (3) the diphosphate moiety makes hydrogen bonds with A146, T320, and S321 (Figure 1b). The 2′ and 3′ hydroxyl groups of the ribofuranose on the nicotinamide side form hydrogen bonds with the carbonyl oxygen atom of acetyl-lysine, which helps to orient the C-1′ atom of NAD for subsequent nucleophilic attack by the peptide *N*-ε-acetyl group.

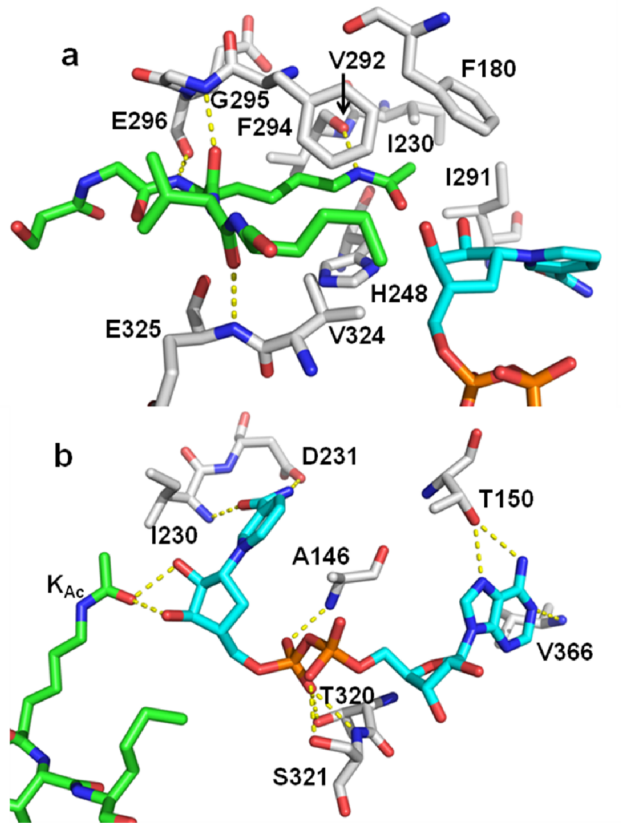

Figure 1. The interactions between the Ac-ACS2 peptide, carba-NAD, and SIRT3. (a) The interface of Ac-ACS2 peptide/SIRT3 interaction. Ac-ACS2 and SIRT3 are shown in stick representation with carbon atoms in green (Ac-ACS2) and white (SIRT3), oxygen atoms in red, and nitrogen atoms in blue. Carba-NAD is visible to the lower right, with carbon atoms in cyan, and phosphorus atoms in orange. (b) The interface of the carba-NAD/SIRT3 interaction. The ACS2 lysine *N*-ε-acetamide is visible on the left side of the figure, with carbon atoms in green.

Ternary Michaelis complex formation brings the acetyl lysine and NAD (**1**) into close proximity so that the key nicotinamide displacement reaction can occur efficiently. According to the proposed catalytic mechanism for sirtuins, the next step after ternary Michaelis complex formation is nucleophilic attack on C-1′ of NAD by the carbonyl oxygen of the substrate *N*-ε-acetyl group. This results in the release of nicotinamide and in the concurrent formation of a 1′-*O*-peptidylamidate-ADPR intermediate, a.k.a., the imidate intermediate. Previously, we determined the structure of SIRT3/imidate intermediate (PDB code 3GLT) by using an ACS2 peptide containing a *N*-ε-thioacetyl lysine, which generates a thioimidate intermediate that remains associated with SIRT3. The thioimidate intermediate is long-lived enough for X-ray diffraction data to be collected on the entire complex.[25] Comparison of the

dx.doi.org/10.1021/jo301067e | J. Org. Chem. 2012, 77, 7319−7329

SIRT3/ACS2/carba-NAD structure with that of the SIRT3/thioimidate intermediate complex revealed a further conformational change after binding of both substrates (Figure 2a). The

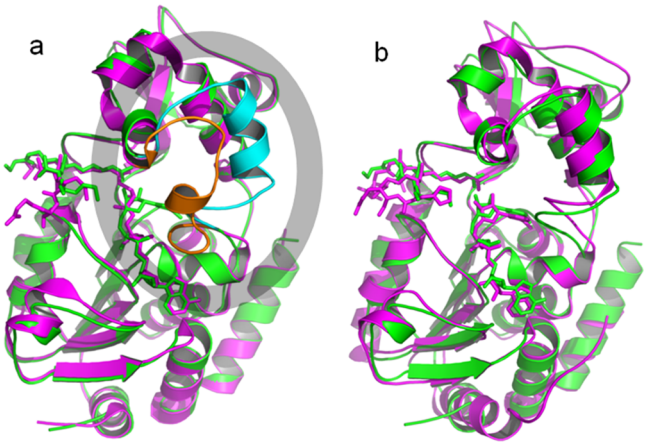

Figure 2. Structural comparison of the SIRT3/ACS2/carba-NAD ternary complex. (a) Comparison of the structure of SIRT3/ACS2/carba-NAD (green/cyan) with that of SIRT3/imidate intermediate (magenta/orange). The cyan-colored helix in the gray oval uncoils to render the orange loop after nicotinamide displacement. (b) Comparison of the structure of SIRT3/ACS2/carba-NAD (green) with that of yHst2/H4/carba-NAD (magenta).

large Rossmann-fold lobes in the two structures are superimposed very well whereas the helix in the connecting loop unwinds and flips down to protect the imidate intermediate from exposure to the solvent. This loop protects the imidate complex from C-1′ nucleophilic attack by water, which would release ADPribose (**4**) but leave the *N*-ε-amide bond intact.

Marmorstein's group has reported a ternary complex structure of the yeast sirtuin yHst2 with a histone H4 peptide and carba-NAD.[17] Comparison of our SIRT3/ACS2/carba-NAD structure with the previously reported yHst2/H4/carba-NAD structure (PDB code 1SZC) shows that the conformations of carba-NAD in the two complexes are very similar and the binding mode is highly conserved in eukaryotes, from yeast to human (Figure 2b).

X-ray Crystal Structure of the SIRT5/IDH2 Peptide/Carba-NAD (9) Ternary Complex. SIRT5 has been reported to have weak deacetylase activity against CPS1, but two recent papers have clearly demonstrated that SIRT5 catalyzes the demalonylation and desuccinylation of peptide and protein substrates both in vivo and in vitro.[26,52,53] It has been demonstrated that lysine 112 of isocitrate dehydrogenase 2 (IDH2) can be desuccinylated by SIRT5. The peptide used in the cocrystallization was a 5-amino acid IDH2 fragment containing succinylated-K112 (Ac-AV-K(Succ)-CA-NH_2). The crystals of SIRT5/Succ-IDH2/**9** ternary complex were obtained by soaking SIRT5/Succ-IDH2 crystals in 10 mM **9** in crystallization solution. Data sets of 2.32 Å and 1.95 Å resolution were collected for crystals of the SIRT5/Succ-IDH2 binary complex and the SIRT5/Succ-IDH2/ **9** ternary complex, respectively.

The IDH2 peptide adopts an extended β-strand conformation, with the main chain amide group forming hydrogen bonds with residues G224, E225, L227 from the small lobe and residue Y255 from the large lobe (Figure 3a). The succinyl lysine side chain is inserted into a deep pocket at the active site, similar to acetyl lysine in other sirtuin structures. The

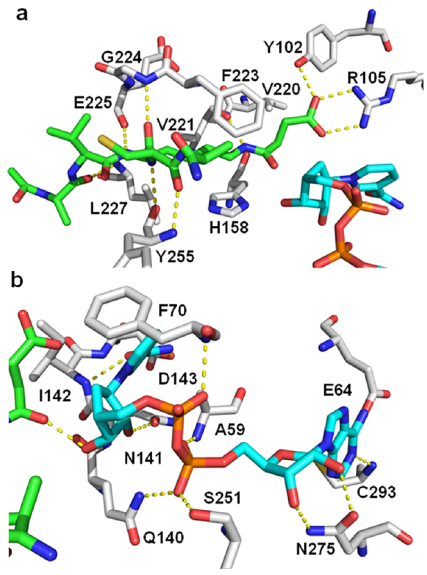

Figure 3. (a) The interface of the IDH2 peptide/SIRT5 interaction. IDH2 and SIRT5 are shown in stick representation with carbon atoms in green (IDH2) and white (SIRT5), oxygen atoms in red, and nitrogen atoms in blue. Carba-NAD is visible to the lower right, with carbon atoms in cyan, and phosphorus atoms in orange. (b) The interface of the carba-NAD/SIRT5 interaction. The IDH2 lysine *N*-ε-acetamide is visible on the left side of the figure, with carbon atoms in green.

methylene units of the succinyl lysine side chain are located in a hydrophobic cavity flanked by V220, V221, and L227. The succinyl group is sandwiched between H158 and F223, with the NH-ε of the succinyl lysine hydrogen bonded with the carbonyl oxygen of V221, which maintains the orientation and the extended conformation of the succinyl lysine side chain. The key determinants in the succinyl lysine binding pocket specificity are R105 and Y102. The bidentate guanidinium side chain of R105 makes a salt bridge with the carboxylate group of the succinyl lysine. In addition, the hydroxyl group of Y102 is hydrogen bonded to the carboxylate of the succinyl lysine. For malonylated peptides, the specificity is presumably mainly determined by the salt bridge between R105 and the carboxylate of the malonyl lysine because the hydrogen bonding with Y102 may not be present unless local conformational changes occur.

Upon soaking carba-NAD (**9**) into the SIRT5/Succ-IDH2 crystals, we observed some similarities between the SIRT5 and SIRT3 ternary complexes. Carba-NAD makes multipoint contacts with SIRT5: (1) the adenine ring forms hydrogen bonds with E64 and C293; (2) the amide group of the nicotinamide ring makes hydrogen bonds with I142 and D143 in the nicotinamide binding C pocket; (3) the pyrophosphate group makes hydrogen bonds with A59, F70, Q140, and S251 (Figure 3b). However, unlike SIRT3, additional interactions between SIRT5 and the two ribose rings are observed: (1) The 2′ hydroxyl group of the ribose ring on the nicotinamide side forms a hydrogen bond with N141. (2) The 2′ and 3′ hydroxyl groups of the ribose ring on the adenine side form hydrogen bonds with N275. This is consistent with our observation that SIRT5 has a K_m for NAD lower than that of SIRT3. As with the SIRT3 complex, the 3′ hydroxyl group of the ribose on the nicotinamide side forms a hydrogen bond with the *N*-ε-

dx.doi.org/10.1021/jo301067e | J. Org. Chem. 2012, 77, 7319−7329

carbonyl oxygen of succinyl lysine, which helps to position NAD C-1′ for nucleophilic attack.

Comparison of our SIRT5/succinyl-IDH2 peptide/carba-NAD crystal structure with the SIRT5/succinyl-H3 peptide/NAD structure previously reported by Lin's group shows that carba-NAD and NAD occupy the same space in both complexes (Figure 4).[26] In particular, the site where NAD (**1**) is substituted to render carba-NAD (**9**) shows no difference in position or orientation.

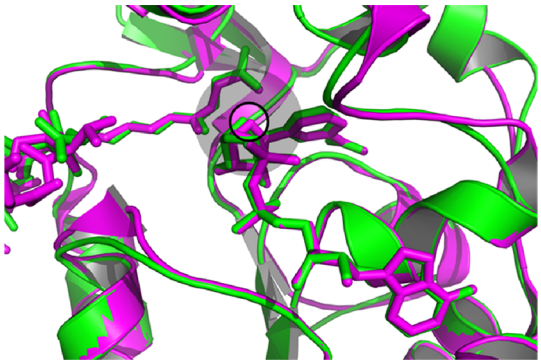

Figure 4. Comparison of the SIRT5/Succ-IDH2 peptide/carba-NAD structure (green) with the SIRT5/Succ-H3K9 peptide/NAD complex (magenta). The center of the gray torus highlights the CH_2 and O overlap between carba-NAD and NAD.

DISCUSSION

The reduction of ester **13** to alcohol **10** was more challenging than we anticipated it would be when we began our synthesis. Different hydride reagents, mainly borohydrides, have been described to reduce ester **13** to alcohol **10**. When we attempted to prepare alcohol **10**, we encountered two major difficulties. First, the reaction often stalled before all of the ester had been consumed. This was due to the poor solubility of **13** in ethereal solvents. We screened both protic and polar, aprotic solvents in the hope of finding a suitable medium for the reduction, but all others proved to be inferior to ethers, either quenching the reducing agent or giving complex mixtures of products. We also made the free amine from the hydrochloride salt, but this did not improve the ether solubility significantly. Historically, the solubility issue has been addressed by the installation of one or more hydrophobic protecting groups on **13**, often an acetal, an amide, or a carbamate. Because this would lengthen the synthesis, we sought to avoid the use of a protecting group if possible. A second problem was that when reduction did occur, the product was invariably complexed with boron. None of the literature procedures described a robust method for dissociation of the boron complex, and the complex proved to be extremely resistant to hydrolysis under both acidic and basic conditions. Using lithium triethylborohydride as the reducing agent, we found that the starting amino ester hydrochloride formed a THF-soluble complex, and ester reduction proceeded to completion.[12,38,41,42] The hydrofluoric acid workup we employed broke the complex between the product and the boron-based reducing agent. It is noteworthy that boronic ester derivatives are commonly used to facilitate dissolution of carbohydrates in organic solvents. Borate esters with carbohydrates hydrolyze in aqueous solution, and are generally not difficult to remove.[54] The boron complex formed upon reduction of **13** with lithium triethylborohydride is probably not a boronic ester but rather a tetracoordinate boron complex. The lack of an open coordination site on the boron atom renders the complex much more stable to hydrolysis than the corresponding boronic ester. Nevertheless, the tetracoordinate complex is susceptible to nucleophilic attack by fluoride. When combined with a hydrofluoric acid workup, trialkylboron complexation may represent an attractive strategy for carbohydrate chemistry that requires an aprotic medium.

The most challenging transformation of the synthesis was the pyrophosphate coupling.[20,21] Many literature methods for preparing pyrophosphates give variable yields, and isolated yields often do not exceed 20%. The major difficulty with these methods lies in the poor solubility of the coupling partners in an anhydrous medium.[55] Our pyrophosphate coupling protocol was a modification of the procedure outlined by Lee.[23] The addition of pyridinium tosylate was a key improvement to the original procedure, as a buffering agent made the coupling yields higher and more consistent from run to run than the previously reported manganese(II)-mediated pyrophosphate coupling methods. Chromatography over an amine-functionalized silica gel column allowed for isolation of carba-NAD (**9**) in a respectable 58% yield. Amine-functionalized silica gel columns were superior to polystyrene-based resins for the isolation of carba-NAD (**9**). Because the silica gel columns are compatible with either organic or aqueous solvents, the crude reaction mixture can be injected directly onto the column and then eluted with acetic acid in methanol to remove the reaction solvent and methanol-soluble reaction components such as pyridine and *N*,*N*′-dicyclohexylguanidine. *p*-Toluenesulfonate is negatively charged and remained bound to the column during the acetic acid in methanol elution, but a sodium acetate buffer in methanol served to elute *p*-toluenesulfonate. Because **9** is insoluble in methanol, it was retained on the column. Subsequent elution with aqueous acetate buffers then recovered **9** from the column. During this separation, amine-linked silica gel columns gave peak resolution better than that of polystyrene-based columns. The purity and yield of the dinucleotide were similar over several runs, and the pyrophosphate coupling and purification sequence can be adapted to prepare other dinucleotides.

Both SIRT3 and SIRT5 are potential therapeutic targets for several human diseases, and we are interested in finding agents to modulate the function of these enzymes. Ternary complexes of each enzyme in complex with a peptide substrate and carba-NAD (**9**) provide snapshots of the enzyme conformations during the catalytic cycle. With ample supplies of carba-NAD on hand, it is possible to obtain structural information for different peptide substrates and with different enzyme constructs. The rational design of ligands that either disrupt or stabilize ligand binding to SIRT3 and SIRT5 is also facilitated by access to X-ray crystal structures of the ternary complexes. Carba-NAD will be an important tool for interrogating the biochemistry of the sirtuins, especially for strategies based on X-ray crystallography. In contrast to NAD-containing complexes, carba-NAD-containing complexes are not subject to catalytic turnover at ambient temperature. The lack of chemical reactivity makes structural work with **9** technically much easier than work with **1**. Ambient temperature soaking or cocrystallization is possible with **9** but would be difficult with **1**. This property should be recapitulated in structural work with other NAD-consuming enzymes.

dx.doi.org/10.1021/jo301067e | J. Org. Chem. 2012, 77, 7319−7329

CONCLUSION

In conclusion, synthetic carba-NAD (**9**) proved to be a good NAD mimetic that bound to SIRT3 or SIRT5, along with an acyl peptide substrate, and provided enzyme−substrate complexes that were chemically stable at ambient temperature. This allowed us to generate X-ray crystal structures of both SIRT3 and SIRT5 ternary complexes with **9** and peptide substrates, providing important insight into each enzyme's mechanism of action. This structural information will aid in the design of agents that modulate SIRT3 and SIRT5 function, with the ultimate goal of developing new treatments for a variety of human diseases. Our synthesis of carba-NAD proceeds in only six linear steps, and seven total steps, starting from the commercially available *R*-(−)-Vince lactam (**11**). No protecting groups were used in this synthesis. A fluoride workup of a $LiEt_3BH$-mediated ester reduction returned a carbohydrate-like substrate without chromatography and without a separate protection−deprotection sequence. In the final synthetic step, our pyrophosphate coupling gave yields much better than those of many common pyrophosphate bond-forming reactions. Because the coupling method is compatible with unprotected carbohydrates, it can be used as the final step to prepare dinucleotides, eliminating the need for additional manipulations to remove protecting groups. This strategy addresses a key obstacle in NAD analogue design and makes the synthesis of NAD analogues a much more tractable pursuit. Wider access to carba-NAD will aid the study of NAD-dependent enzymes. A practical method for preparing NAD analogues opens new avenues for the investigation of enzymes and biochemical pathways found in all living organisms. This may offer new insights into chemistry and biochemistry that appeared very early in the history of life on earth.

EXPERIMENTAL SECTION

General. Reagents were purchased from commercial sources and used without further purification. LCMS data were obtained using a C-18 column and a gradient of 5 to 100% CH_3CN in 0.1% (v/v) formic acid:water. Unfunctionalized silica gel column chromatography was performed using an automated medium-pressure liquid chromatography system. ^1H NMR spectra were recorded at 300 MHz. Chemical shift data are reported in parts per million, with tetramethylsilane at 0.00 ppm. Information for each resonance is reported in the following order: chemical shift (multiplicity, integration, coupling constants (if any), and proton assignments.) Spectral multiplicity abbreviations are as follows: s, singlet; d, doublet; t, triplet; dd, doublet of doublets; dt, doublet of triplets; m, multiplet. Integration refers to the number of protons per signal. Proton-decoupled ^{13}C spectra were recorded at 75 MHz. Chemical shift data are reported in parts per million, with tetramethylsilane at 0.00 ppm. Information for each resonance is reported in the following order: chemical shift (carbon assignment, number of hydrogens attached (if any)). Where carbon−phosphorus couplings are reported, the coupling constant is designated as J_{C-P}. High resolution mass spectra were recorded in positive ion mode using electrospray ionization and a time-of-flight mass analyzer. Melting points were determined using an open capillary tube with a heating block apparatus and optical observation.

Ion Chromatography. Ion chromatography was performed using an automated medium-pressure liquid chromatography system. Commercially available prepacked aminopropyl-linked silica gel columns were used for chromatography. New columns were conditioned by washing with 1 M sodium acetate and 1 M acetic acid in water (five column volumes), followed by 1 M aqueous acetic acid (five column volumes) once daily for one week, and then every three days until no resin appeared in the column effluent. Two weeks was usually sufficient to condition a column. Columns were stored in 1 M aqueous acetic acid at ambient temperature between washes. Immediately prior to use, the columns were flushed with two volumes of the first solvent to be used for chromatography. Following ion chromatography, columns were washed with 1 M sodium acetate/1 M acetic acid until no UV absorbing material eluted from the column, and then the columns were washed with either 1 M aqueous acetic acid or 0.1 M acetic acid in methanol and stored at ambient temperature. Chromatograms were monitored by absorbance at 254 nm for nucleotide elution and by conductivity for salt elution.

Carba-NAD (9), 1-((1*R*,2*S*,3*R*,4*R*)-4-(((((((2*R*,3*S*,4*R*,5*R*)-5-(6-Amino-9*H*-purin-9-yl)-3,4-dihydroxytetrahydrofuran-2-yl)-methoxy)hydroxyphosphoryl)oxy)oxidophosphoryl)oxy)-methyl)-2,3-dihydroxycyclopentyl)-3-carbamoylpyridin-1-ium. To a mixture of 150 mg (0.388 mmol) of **16**, 551 mg (0.776 mmol) of adenosine 5-monophosphomorpholidate 4-morpholine-N,*N*-dicylcohexylcarboxamidine salt, 200 mg (1.05 mmol) of *p*-toluenesulfonic acid monohydrate, and 146 mg (1.16 mmol) of anhydrous $MnCl_2$ were added 0.4 mL (5 mmol) of pyridine and 2 mL of formamide. The reaction was stirred at ambient temperature under N_2 for 20 h. HPLC/MS showed that the AMP morpholidate was completely consumed after this time.

A 47 g amine-functionalized silica gel column was equilibrated with 0.1 M acetic acid in methanol. The reaction was transferred to a syringe, and then the reaction flask was washed with 6 drops of water. The washings were added to the syringe containing the reaction mixture, and then the entire contents were loaded onto the column. The column was eluted at 30 mL/min with the following sequence of solvents: (1) 250 mL of 0.1 M acetic acid in methanol (to recover the morpholinecarboxamidine salt, formamide, and pyridine as a single peak), (2) 300 mL of 0.1 M acetic acid and 0.1 M sodium acetate in methanol (to recover sodium *p*-toluenesulfonate), (3) 150 mL of 0.1 M acetic acid in methanol (to remove sodium acetate from the column), (4) 200 mL of 0.1 M aqueous acetic acid (to recover a small amount of unreacted **16** and some $MnCl_2$), (5) 200 mL of 0.01 M aqueous acetic acid (to reduce the concentration of acetic acid on the column), and (6) 200 mL of 0.15 M sodium acetate/0.01 M acetic acid in water (to recover carba-NAD (**9**)). Adenosine monophosphate began to elute as a broad peak after the carba-NAD peak. The column was washed with 1 M sodium acetate and 1 M acetic acid in water to remove the rest of the reaction byproducts (including adenosine monophosphate and some diadenosine dinuclotide) as a single UV active peak. The column was then equilibrated with 0.1 M acetic acid in methanol.

The carba-NAD fraction was concentrated in vacuo at 40 °C until sodium acetate began to crystallize (residual volume about 2 mL). The residue was dissolved in 10 mL of methanol, and then 1 mL of 0.5 M EDTA in water (pH = 8) was added to sequester traces of Mn^{2+}. The solution was concentrated in vacuo to remove as much of the water as possible, and then the residue was taken up in 10 mL of methanol and injected onto a 47 g amine-functionalized silica gel column, equilibrated with 0.1 M acetic acid in methanol. The column was eluted at 30 mL/min with 300 mL of 0.1 M acetic acid in methanol (to recover sodium acetate) and then with 300 mL of 1 M acetic acid in water (to recover carba-NAD). The column was washed with 1 M sodium acetate and 1 M acetic acid in water and then with 0.1 M acetic acid in methanol and stored in 0.1 M acetic acid in methanol. The carba-NAD-containing fraction was concentrated in vacuo at 40 °C to a thick, colorless oil. This was taken up in water and concentrated in vacuo (3 × 5 mL) to remove the remaining acetic acid. The oily residue was then taken up in 5 mL of water, frozen, and lyophilized to give 160 mg (58%) of **9** as a colorless, amorphous solid. Carba-NAD (**9**) remained a solid after storing for several weeks at ambient temperature and humidity. As a precaution, it was stored at −20 °C in a glass vial. Spectral data were in agreement with those of Slama and Simmons.[12] ^1H NMR (D_2O) δ 9.40 (s, 1H, H2), 9.18 (d, 1H, J = 6.3 Hz, H4), 8.91 (d, 1H, J = 8.1 Hz, H6), 8.60 (s, 1H, H8‴), 8.41 (s, 1H, H2‴), 8.23 (dd, 1H, J = 8.1, 6.3 Hz, H5), 6.12 (d, 1H, J = 5.3 Hz, H1″), 5.09 (q, 1H, J = 9.5 Hz, H1′), 4.72 (t, 1H, J = 5.3 Hz, H2″), 4.52 (m, 2H, H3″, H2′), 4.39 (m, 1H, H4″), 4.32−4.11 (m, 4H, H3′, H5″a, H5″b, H5′a), 4.07 (m, 1H, H5′b), 2.72 (dt, 1H, J = 13.3, 8.8 Hz, H6′α(cis to OH)), 2.46 (m, 1H, H4′), 2.21 (ddd, 1H, J = 13.3,

dx.doi.org/10.1021/jo301067e | J. Org. Chem. 2012, 77, 7319−7329

10.3, 7.7 Hz, H6′β(trans to OH)); ^{13}C NMR (D_2O) δ 166.15 (C7), 150.61 (C6‴), 148.82 (C4‴), 146.25 (C4-H), 145.85 (C6-H), 145.65 (C2‴-H), 143.58 (C2-H), 142.82 (C8‴-H), 134.61 (C3), 129.31 (C5), 118.90 (C5‴), 88.47 (C1″-H), 84.81 (d, J_{C-P} = 8.8 Hz, C4″-H), 77.70 (C2′-H), 76.52 (C1′-H), 75.37 (C2″-H), 72.84 (C3′-H), 70.85 (C3″-H), 67.44 (d, J_{C-P} = 6.1 Hz, C5′-H), 65.77 (d, J_{C-P} = 4.3 Hz, C5″-H), 43.75 (d, J_{C-P} = 8.7 Hz, C4′-H), 29.47 (C6-H_2); HR-MS (ESI) m/z ([M + H]$^+$) calcd for $C_{22}H_{30}N_7O_{13}P_2$ 662.1377, found 662.1379.

(1*R*,2*S*,3*R*,5*R*)-3-Amino-5-(hydroxymethyl)cyclopentane-1,2-diol (10). A 500 mL round-bottomed flask was charged with 4.50 g (21.3 mmol) of **13**. To the solid was added 45 mL of anhydrous THF. The flask was placed under N_2 and cooled with an ice bath. To the suspension was added 106 mL of a 1 M solution of lithium triethylborohydride in THF, slowly, to control the evolution of gas. The suspension gradually became clear over the course of the addition. After addition was complete, the reaction mixture was stirred with ice-cooling for 30 min. Next, a stream of nitrogen was introduced to sweep the reaction headspace. While the reaction was purged with N_2, 100 mL of water was added and the solvent was evaporated in vacuo at 40 °C to give a white oil. An additional 50 mL of water was added and evaporated again to remove residual THF. The white oil was resuspended in 50 mL of water and cooled with an ice bath. While the suspension was purged with N_2, 110 mL of a 2.5 M aqueous hydrofluoric acid solution was cautiously added, and then the mixture was stirred for 10 min. (The HF addition generates ethane, and the N_2 sweep must remove the ethane as it forms to avoid the danger of a flash fire.) The solvent was evaporated in vacuo at 40 °C to give a white oil. The residue was suspended in 10 mL of water, and then 70 mL of acetonitrile was added. Two layers separated, and the top layer was decanted. The bottom layer was suspended in 5 mL of water, and 35 mL of acetonitrile was added. Two layers separated, and the top layer was decanted. The combined top layers were allowed to stand at ambient temperature for 3 days, after which time a bottom layer separated. The bottom layers from all of the acetonitrile extractions were combined and the solvent was evaporated in vacuo at 40 °C to give a white oil. The oil was suspended in 5 mL of water, and 35 mL of acetonitrile was added. Two layers separated, and the top layer was decanted. The remaining oil was suspended in 50 mL of water. A 3 M aqueous lithium hydroxide solution was added to bring the suspension to pH = 13. The suspension was filtered to remove a white precipitate of LiF, and then the filtrate was evaporated in vacuo at 40 °C. Next, 50 mL of ethanol was added to the oily residue, and the mixture was allowed to stand overnight. The suspension was transferred to centrifuge tubes with the aid of 50 mL of ethanol and 100 mL of methanol. The tubes were centrifuged at 3000 rpm for 5 min. The supernatant was decanted. The remaining solids in the tubes were suspended in 80 mL of methanol and centrifuged again. The combined supernatants were evaporated in vacuo at 40 °C to give a clear, colorless oil. The oil was dissolved in 50 mL of ethanol and filtered through a 0.2 μm filter. The filtrate was evaporated in vacuo at 40 °C, 50 mL of water was added, and the solution was concentrated in vacuo to drive off the remaining ethanol. The remaining oil was dried in vacuo at ambient temperature to give 4.16 g of **10** as a light, yellow oil. Karl Fischer titration showed 25.2% H_2O by weight, for a yield of 3.12 g (99%). Spectral data (in CD_3OD) were in agreement with those reported by Madhaven.[37] Spectral assignments of H4α and H4β were in accordance with Abraham.[56] ^{1}H NMR (D_2O) δ 3.81 (t, 1H, J = 5.0 Hz, H1), 3.55 (m, 3H, H2 and CH_2O), 3.09 (dt, 1H, J = 8.8, 7.5 Hz, H3), 2.12 (m, 1H, H4α(cis to OH)), 2.02 (m, 1, H5), 0.95 (dt, 1H, J = 12.6, 8.8 Hz, H4β(trans to OH)); ^{13}C NMR δ 78.74 (C2-H), 72.90 (C1-H), 63.55 (CH_2O), 54.69 (C3-H), 44.55 (C5-H), 31.22 (C4-H_2). HR-MS (ESI) m/z ([M + H]$^+$) calcd for $C_6H_{14}NO_3$ 148.0974, found 148.0972.

(1*R*,4*S*,5*R*,6*S*)-5,6-Dihydroxy-2-azabicyclo[2.2.1]heptan-3-one (12). To a solution of 4.33 g (39.7 mmol) of (1*R*,4*S*)-2-azabicyclo[2.2.1]hept-5-en-3-one (*R*-(−)-Vince lactam (**11**)) and 5.14 g (43.9 mmol) of *N*-methylmorpholine *N*-oxide in 20 mL of isoamyl alcohol and 20 mL of water in a resealable tube was added 3 mL (0.24 mmol) of 2.5% (w/w) OsO_4 in *tert*-butyl alcohol. The tube was sealed with a PTFE cap, and the reaction was heated at 70 °C for 1−4 h. TLC (20% i-PrOH/80% EtOAc, silica gel plate, $KMnO_4$ or *p*-anisaldehyde stain) showed complete consumption of the starting material after this time. (Additional OsO_4 solution could be added if any starting material remained. Minimal reaction headspace eliminated the need for more OsO_4.) Heating was removed, 500 mg (4.81 mmol) of $NaHSO_3$ was added, and the mixture was stirred for 45 min while cooling to ambient temperature. The solvents were removed in vacuo at 40 °C. The thick, dark brown, oily residue was suspended in 30 mL of methanol and 30 mL of 2-propanol was added. The mixture was concentrated in vacuo to remove as much water and *N*-methylmorpholine as possible, giving a brown solid. This solid was suspended in 50 mL of methanol, slurried with 50 mL of silica gel, and concentrated to dryness in vacuo at 40 °C. A 120 g silica gel column was equilibrated with 10% 2-propanol/90% ethyl acetate, and the silica gel product mixture was fitted to the top of the column. The column was eluted at a rate of 85 mL/min with 10% i-PrOH/EtOAc for 5 min, a 10% to 30% i-PrOH/EtOAc gradient over 20 min, and then 30% i-PrOH/EtOAc for 5 min. The product eluted at about 20% i-PrOH/EtOAc and gave a very weak UV absorbance at 254 nm. TLC (20% i-PrOH/EtOAc, stain with freshly prepared *p*-anisaldehyde stain) showed that the undesired all-cis isomer eluted first and gave a pink spot, while the desired isomer followed closely and displayed a yellow spot which turned brown on further heating. The product-containing fractions were concentrated in vacuo at 30−40 °C to give a white solid. This material was taken up in 20 mL of hot methanol and concentrated in vacuo to remove the residual chromatography solvents, to give 4.27 g (75%) of the product as a white, crystalline solid, mp 152−153 °C. ^{1}H NMR data were in agreement with those of Oppenheimer.[41] ^{1}H NMR (D_2O) δ 4.06 (dd, 1H, J = 5.9, 0.7 Hz, H5), 4.01 (dd, 1H, J = 5.9, 0.7 Hz, H6), 3.78 (m, 1H, H1), 2.62 (m, 1H, H4), 2.07 (m, 2H, H7); ^{13}C NMR (D_2O) δ 182.0 (C3), 71.7 (C6-H), 68.4 (C5-H), 59.3 (C1-H), 51.9 (C4-H), 36.3 (C7-H_2); HR-MS (ESI) m/z ([M + H]$^+$) calcd for $C_6H_{10}NO_3$ 144.0661, found 144.0661.

(1*S*,2*R*,3*S*,4*R*)-Methyl 4-Amino-2,3-dihydroxycyclopentanecarboxylate Hydrochloride (13). To 2.10 g of **12** was added 25 mL of methanol. The mixture was heated gently to dissolve the starting material, and then $HCl_{(g)}$ was added until saturated. The solution was stirred at ambient temperature for 18 h, while monitoring by LCMS for the disappearance of starting material and the appearance of a more polar product. The solution was concentrated in vacuo to give 3.07 g (99%) of a white, crystalline solid, mp 179−180 °C. Spectral data were in agreement with those of Slama and Simmons.[12] ^{1}H NMR (D_2O) δ 4.29 (t, 1H, J = 5.4 Hz, H2), 4.07 (dd, 1H, J = 7.2, 5.4 Hz, H3), 3.74 (s, 3H, H7), 3.57 (q, 1H, J = 8.3 Hz, H4), 3.00 (dt, 1H, J = 9.0, 5.0 Hz, H1), 2.52 (dt, 1H, J = 13.8, 8.6 Hz, H5α-cis to OH), 1.85 (dt, 1H, J = 13.8, 9.2 Hz, H5β-trans to OH); ^{13}C NMR (D_2O) δ 175.36 (C6), 74.17 (C3-H), 72.62 (C2-H), 54.45 (C4-H), 52.78 (C7-H_3), 47.56 (C1-H), 27.18 (C5-H_2). HR-MS (ESI) m/z ([M + H]$^+$) calcd for $C_7H_{14}NO_4$ 176.0922, found 176.0923.

3-Carbamoyl-1-((1*R*,2*S*,3*R*,4*R*)-2,3-dihydroxy-4-(hydroxymethyl)cyclopentyl)pyridin-1-ium Chloride (14). To a solution of 3.06 g (74.8% by weight, 15.5 mmol) of **10** in 12 mL of methanol at ambient temperature was added a solution of 4.86 g (15.0 mmol) of **15** in 12 mL of methanol. The reaction immediately turned red-violet. Next, 1.23 g (15.0 mmol) of sodium acetate was added, and the reaction was stirred at ambient temperature for 2 h. To remove any traces of excess pyridinium salt **15**, 1 mL of 17 M $NH_4OH_{(aq)}$ was added and the reaction was stirred for 10 min. The solvents were removed in vacuo, and the residue was suspended in water and filtered to remove 2,4-dinitroaniline. The filtrate was concentrated in vacuo to an oil. This was dissolved in methanol and concentrated again to remove residual water. The oily residue was taken up in methanol and loaded onto a 120 g silica gel column. The column was eluted with a mixture of A = ethyl acetate and B = 5% (v/v) acetic acid in methanol, eluting with 120 mL of 95: 5 A: B and then a gradient of 95: 5 A: B to 100% B over 480 mL and finally 960 mL of B. The product-containing fractions were combined and concentrated in vacuo. The residue was taken up in 100 mL of water, concentrated in vacuo two times, and then dissolved in 50 mL of water, and 0.5 mL of 12 M $HCl_{(aq)}$ was

dx.doi.org/10.1021/jo301067e | J. Org. Chem. 2012, 77, 7319−7329

added. The solution was concentrated in vacuo, and then the residue was taken up in 100 mL of methanol, concentrated in vacuo two times, and then dried under high vacuum at ambient temperature for 18 h. This gave 3.32 g (76%) of **14** as a yellow hygroscopic foam, containing 1 wt % methanol by ^{1}H NMR. The product was kept protected from atmospheric moisture for use in the subsequent phosphorylation step. Spectral data were in agreement with those of Slama and Simmons.[12] Assignment of some ^{1}H NMR signals was by analogy to Abraham and Moinuddin.[56,57] ^{1}H NMR (D_2O) δ 9.40 (s, 1H, H2), 9.15 (dt, 1H, J = 6.2, 1.1 Hz, H6), 8.95 (dt, 1H, J = 8.1, 1.5 Hz, H4), 8.25 (dd, 1H, J = 8.0, 6.3 Hz, H5), 5.09 (ddd, 1H, J = 10.8, 9.4, 8.0 Hz, H1′), 4.44 (dd, 1H, J = 9.4, 6.0 Hz, H2′), 4.11 (dd, 1H, J = 5.9, 3.1 Hz, H3′), 3.75 (d, 2H, J = 5.9 Hz, H5′), 2.70 (dd, 1H, J = 13.2, 8.2 Hz, H6α′(cis to OH)), 2.34 (m, 1H, H4′), 1.99 (ddd, 1H, J = 13.2, 11.0, 8.6 Hz, H6β′(trans to OH)); ^{13}C NMR (D_2O) δ 166.45 (C7), 146.03 (C6-H), 145.41 (C4-H), 143.77 (C2-H), 138.80 (C3), 129.24 (C5-H), 77.36 (C2′-H), 76.22 (C1′-H), 72.20 (C3′-H), 63.24 (C5′-H), 44.61 (C4′-H), 29.19 (C6′-H_2); HR-MS (ESI) m/z ([M + H]$^+$) calcd for $C_{12}H_{17}N_2O_4$ 253.1188, found 253.1187.

3-Carbamoyl-1-(2,4-dinitrophenyl)pyridin-1-ium Chloride (15). A 100 mL round-bottomed flask was charged with 6.07 g (30.0 mmol) of 2,4-dinitrochlorobenzene and 3.66 g (30.0 mmol) of nicotinamide (**3**). The reaction was heated at 100 °C for 20 min with magnetic stirring. The solids melted to give a homogeneous liquid, and then the mixture hardened and became difficult to stir. Heating was removed, and the mixture was cooled to ambient temperature to give a dark orange glass. This was dissolved in 50 mL of methanol, and then 75 mL of silica gel was added, adding more methanol if necessary to suspend all of the silica gel. The mixture was concentrated to dryness in vacuo, using heptanes to chase the last traces of methanol from the mixture. A 120 g prepacked silica gel column was equilibrated with 20% CH_3OH/80% CH_2Cl_2, the silica gel mixture was fitted to the top of the column, and the column was eluted with 20% CH_3OH/CH_2Cl_2 for 5 min at a rate of 85 mL/min to remove unreacted dinitrochlorobenzene. A gradient of 20% CH_3OH/80% CH_2Cl_2 to 40% CH_3OH/60% CH_2Cl_2 over 25 min was run, followed by 40% CH_3OH/60% CH_2Cl_2 for 5 min. During the gradient, nicotinamide eluted, followed closely by the product. The product-containing fractions were concentrated in vacuo to 5.99 g (58%) of a yellow foam, containing 0.66 mol CH_3OH/1 mol product. Attempts to crystallize this material from various solvents were unsuccessful, but the amorphous solid could be stored for several months under ambient conditions. ^{1}H NMR (D_2O) δ 9.67 (m, 1H, H2), 9.40 (d, 1H, J = 2.5 Hz, H3′), 9.34 (dt, 1H, J = 6.1, 1.3 Hz, H6), 9.27 (dt, 1H, J = 8.2, 1.3 Hz, H4), 8.95 (dd, 1H, J = 8.6, 2.5 Hz, H5′), 8.49 (ddd, 1H, J = 8.2, 6.1 0.5 Hz, H5), 8.26 (d, 1H, J = 8.6 Hz, H6′). ^{13}C NMR (D_2O) δ 165.6 (C7), 150.4 (C2′), 148.1 (C6-H), 147.9 (C4-H), 146.3 (C2-H), 143.4 (C4′), 139.0 (C1′), 134.8 (C3), 131.7 (C6′-H), 131.4 (C5′-H), 129.2 (C5-H), 123.4 (C3′-H). HR-MS (ESI) m/z ([M + H]$^+$) calcd for $C_{12}H_9N_4O_5$ 289.0573, found 289.0573.

((1*R*,2*R*,3*S*,4*R*)-4-(3-Carbamoylpyridin-1-ium-1-yl)-2,3-dihydroxycyclopentyl)methyl Hydrogen Phosphate (16). Immediately prior to use, 500 mg (1.64 mmol) of **14** was dissolved in 5 mL of methanol and then concentrated in vacuo to give a pale yellow foam. The foam was dissolved in 5 mL of methanol and concentrated in vacuo a second time, and then the resulting foam was dried under high vacuum (<1 Torr) and at ambient temperature for 30 min to give anhydrous **14**, containing approximately 0.6 equiv of residual methanol as determined by ^{1}H NMR integration. This was suspended in 4 mL of freshly distilled trimethyl phosphate, and the suspension was stirred for 1 min under high vacuum at ambient temperature to remove a small amount of volatile material. The reaction flask was backfilled with N_2 and then cooled with an ice bath. Next, 450 μL (4.92 mmol) of $POCl_3$ was added via syringe. The starting material dissolved over 5 min after the $POCl_3$ had been added. The reaction was stirred with ice cooling for 1 h, and then 2 mL of water was added. This was stirred for 40 min while cooling with an ice bath, and then the reaction was diluted into a solution of 2.00 g (24.4 mmol) of sodium acetate in 125 mL of methanol at ambient temperature.

A 47 g amine-functionalized silica gel column was equilibrated with 0.1 M acetic acid in methanol. The reaction mixture in methanol was injected onto this column at a rate of 30 mL/min. During the injection, the product was retained while trimethyl phosphate, sodium acetate, and any unreacted **14** eluted from the column. The column was then eluted with 200 mL of 0.1 M acetic acid in methanol (30 mL/min) to remove the remaining methanol-soluble reaction components. Next, the column was eluted with 200 mL of 0.1 M aqueous acetic acid (30 mL/min) to recover the product. The column was washed with 300 mL of 1 M sodium acetate and 1 M acetic acid in water and then with 200 mL of 0.1 M acetic acid in methanol and stored in 0.1 M acetic acid in methanol. The product containing fractions were combined and concentrated in vacuo at 40 °C to give an oily residue. This was taken up in water and concentrated (2 × 5 mL) to remove most of the remaining acetic acid. The residue was taken up in 5 mL of water, frozen, and lyophilized to give 480 mg (76%) of a pale yellow amorphous solid. This foam was not appreciably hygroscopic upon handling at ambient temperature and humidity and could be stored in a capped glass vial for several months. Spectral data were in agreement with those of Slama and Simmons.[12] Assignment of some ^{1}H NMR signals was by analogy to Abraham and Moinuddin.[56,57] ^{1}H NMR (D_2O) δ 9.39 (t, 1H, J = 1.4 Hz, H2), 9.18 (dd, 1H, J = 6.3, 1.2 Hz, H6), 8.94 (dd, 1H, J = 8.1, 1.4 Hz, H4), 8.24 (dd, 1H, J = 8.0, 6.3 Hz, H5), 5.10 (td, 1H, J = 9.8, 8.7 Hz, H1′), 4.49 (dd, 1H, J = 9.6, 5.7 Hz, H2′), 4.19 (dd, 1H, J = 5.7, 2.4 Hz, H3′), 4.06 (ddd, 1H, J = 10.2, 5.0, 4.7 Hz, H5′a), 3.96 (ddd, 1H, J = 10.2, 5.0, 4.7 Hz, H5′b), 2.74 (dt, 1H, J = 13.6, 8.6 Hz, H6′α(cis to OH)), 2.45 (m, 1H, H4′), 2.13 (ddd, 1H, J = 13.4, 10.6, 7.8 Hz, H6′β(trans to OH)); ^{13}C NMR (D_2O) δ 166.36 (C7), 146.07 (C6-H), 145.58 (C4-H), 143.78 (C2-H), 134.68 (C3), 129.32 (C5-H), 77.83 (C2′-H), 76.56 (C1′-H), 73.07 (C3′-H), 65.89 (d, J_{C-P} = 5.2 Hz, C5′-H), 43.15 (d, J_{C-P} = 8.1 Hz, C4′-H), 29.70 (C6′-H_2); HR-MS (ESI) m/z ([M + H]$^+$) calcd for $C_{12}H_{18}N_2O_7P$ 333.0852, found 333.0853.

Crystallization and Structural Determination of SIRT3 Complex. SIRT3/ASC2 crystals were obtained by the hanging drop vapor diffusion method at 18 °C. The drop was composed of 1 μL of the protein/peptide mixture and 1 μL of the crystallization buffer containing 0.2 M Li_2SO_4, 15% (w/v) polyethylene glycol (PEG) 12000, and 0.1 M Bis-Tris, pH 5.3. The SIRT3/ACS2 crystals were then cross-linked by glutaraldehyde and soaked for 1 h in 10 mM carba-NAD in crystallization buffer.

The SIRT3/ASC2 crystals soaked with carba-NAD (**9**) were cryoprotected in mother liquor containing 20% glycerol and 10 mM carba-NAD (**9**) before being flash-frozen in liquid nitrogen. Diffraction data were collected at APS 21D and processed using the HKL2000 program.[58] The structure was solved by molecular replacement using the structure of SIRT3/ACS2 complex (PDB code 3GLR) as a search model. Detailed information regarding the diffraction data, refinement, and structure statistics is listed in the Supporting Information. All the parameters for each diffraction data set are from that reprocessed by Mosflm[59] and Scala,[60] and refinement statistics are from Refmac[61] in the CCP4[62] suite for consistency.

Crystallization and Structural Determination of SIRT5 Complexes. SIRT5/Succ-IDH2 crystals were obtained by the hanging drop vapor diffusion method at 18 °C. The drop was composed of 1 μL of the protein/peptide mixture and 1 μL of a crystallization solution containing 0.15 M magnesium formate and 20% (w/v) PEG 3350. The SIRT5/Succ-IDH2 crystals were then cross-linked by glutaraldehyde and soaked in 5 mM carbaNAD (**9**) in crystallization solution overnight.

Crystals of SIRT5/Succ-IDH2 cross-linked by glutaraldehyde were soaked in 5 mM carba-NAD (**9**) overnight. The data set was collected at beamline SSRF BL17U. HKL2000 was used to process the data set to 1.95 Å in space group P212121 with two monomers in one asymmetric unit. The molecular replacement software Phaser[63] was used to solve the structure with the search model generated from the monomer structure of the published PDB entry 2NYR. A 2-fold symmetry related dimer solution was successfully obtained, and then iterative structure refinement and model building were performed between Phenix.refine[64] and Coot.[65] In the final refined structure, only

dx.doi.org/10.1021/jo301067e | J. Org. Chem. 2012, 77, 7319−7329

one copy of carba-NAD (**9**) could be observed. Detailed information regarding the diffraction data, refinement, and structure statistics is listed in the Supporting Information.

Protein Cloning, Expression, and Purification of hSIRT3. The 16-residue N-terminal deletion construct of human SIRT3(118−399) was expressed and purified as described previously.[25]

Protein Cloning, Expression, and Purification of hSIRT5. Human SIRT5(34−302) was cloned into a pET28a vector. The protein was expressed in *E. coli* BL21-CodonPlus(DE3)-RIL Cells (Stratagene) as an N-terminal fusion to a hexahistidine affinity tag with an integrated thrombin protease site. A single colony was inoculated in LB media containing 100 μg/mL ampicillin at 37 °C, 250 rpm until the A_{600} reached 0.3. The culture was then transferred to 18 °C, 250 rpm until the A_{600} reached 0.6−0.8. Isopropyl 1-thio-β-D-galactopyranoside was added to a final concentration of 0.5 mM, and expression was continued at 18 °C, 160 rpm overnight. Cells were collected by centrifugation, and the pellet was resuspended in lysis buffer (200 mM NaCl, 5% glycerol, 5 mM 2-mercaptoethanol, and 25 mM HEPES−NaOH, pH 7.5) and then sonicated to break the cells. The supernatant was separated from the cell debris by centrifugation at 10,000*g* for 40 min at 4 °C . The supernatant was loaded onto a Ni-NTA column (Qiagen) that had been equilibrated with a buffer containing 200 mM NaCl, 5% glycerol, 5 mM 2-mercaptoethanol, 20 mM imidazole, and 25 mM HEPES−NaOH, pH 7.5. The column was washed with five column volumes of a buffer containing 200 mM NaCl, 5% glycerol, 5 mM 2-mercaptoethanol, 50 mM imidazole, and 25 mM HEPES−NaOH, pH 7.5 and then eluted with a buffer containing 200 mM NaCl, 5% glycerol, 5 mM 2-mercaptoethanol, 250 mM imidazole, and 25 mM HEPES−NaOH, pH 7.5. The eluted protein was dialyzed against a dialyzing buffer containing 100 mM NaCl, 10% glycerol, 1 mM DTT, and 20 mM HEPES−NaOH, pH7.5, and concentrated. The protein was further purified by a S200 column to 95% purity as assessed by SDS-PAGE analysis stained by Coomassie Brilliant Blue R-250 and concentrated to 10 mg/mL in the dialyzing buffer.

■ ASSOCIATED CONTENT

Supporting Information

^{1}H, ^{13}C, and 2-D NMR spectra and compound numbering schemes for **9**, **10**, **12**−**16**. X-ray crystallographic data processing and refinement parameters. This material is available free of charge via the Internet at http://pubs.acs.org.

Accession Codes

PDB. The access codes for the previously determined structures are as follows: yHST2, 1SZC; SIRT3, 3GLR and 3GLT; SIRT5, 2NYR. The access codes for the SIRT3/ACS2/carba-NAD complex and SIRT5/IDH2/carba-NAD complex are 4FVT and 4G1C, respectively.

■ AUTHOR INFORMATION

Corresponding Author

*E-mail: bruce.2.szczepankiewicz@gsk.com.

Notes

The authors declare no competing financial interest.

■ ACKNOWLEDGMENTS

We thank Thomas Riera for helpful discussions.

■ REFERENCES

(1) Oppenheimer, N. *Mol. Cell. Biochem.* **1994**, *138*, 245−251.
(2) Sauve, A. A.; Wolberger, C.; Schramm, V. L.; Boeke, J. D. *Annu. Rev. Biochem.* **2006**, *75*, 435−465.
(3) Hassa, P. O.; Haenni, S. S.; Elser, M.; Hottiger, M. O. *Microbiol. Mol. Biol. Rev.* **2006**, *70*, 789−829.
(4) Hakmé, A.; Wong, H. K.; Dantzer, F.; Schreiber, V. *EMBO J.* **2008**, *9*, 1094−1100.
(5) Malavasi, F.; Deaglio, S.; Funaro, A.; Ferrero, E.; Horenstein, A. L.; Ortolan, E.; Vaisitti, T.; Aydin, S. *Physiol. Rev.* **2008**, *88*, 841−886.
(6) Cen, Y.; Youn, D. Y.; Sauve, A. A. *Curr. Med. Chem.* **2010**, *18*, 1919−1936.
(7) Hottiger, M. O.; Hassa, P. O.; Lüscher, B.; Schüler, H.; Kock-Nolte, F. *Trends Biochem. Sci.* **2010**, *35*, 208−219.
(8) Sanders, B. D.; Jackson, B.; Marmorstein, R. *Biochim. Biophys. Acta* **2010**, *1804*, 1604−1616.
(9) Hoff, K. G.; Avalos, J. L.; Sens, K.; Wolberger, C. *Structure* **2006**, *14*, 1231−1239.
(10) Liu, Q.; Kriksunov, I. A.; Graeff, R.; Lee, H. C.; Hao, Q. *J. Biol. Chem.* **2007**, *282*, 5853−5861.
(11) Graeff, R.; Liu, Q.; Kriksunov, I. A.; Kotaka, M.; Oppenheimer, N.; Hao, Q.; Lee, H. C. *J. Biol. Chem.* **2009**, *284*, 27629−27636.
(12) Slama, J. T.; Simmons, A. M. *Biochemistry* **1988**, *27*, 183−193.
(13) Slama, J. T.; Simmons, A. M. *Biochemistry* **1991**, *30*, 2527−2534.
(14) Wall, K. A.; Klis, M.; Kornet, J.; Coyle, D.; Ame, J.-C.; Jacobsen, M. K.; Slama, J. T. *Biochem. J.* **1998**, *335*, 631−636.
(15) Slama, J. T.; Simmons, A. M. *Biochemistry* **1989**, *28*, 7688−7694.
(16) Muller-Steffner, H.; Slama, J.; Schuber, F. *Biochem. Biophys. Res. Commun.* **1996**, *228*, 128−133.
(17) Zhao, K.; Harshaw, R.; Chai, X.; Marmorstein, R. *Proc. Natl. Acad. Sci. U.S.A.* **2004**, *101*, 8563−8568.
(18) Sanders, B. D.; Zhao, K.; Slama, J. T.; Marmorstein, R. *Mol. Cell* **2007**, *25*, 463−472.
(19) Haynes, L. J.; Hughes, N. A.; Kenner, G. W.; Todd, A. R. *J. Chem. Soc.* **1957**, 3727−3732.
(20) Furusawa, K.; Sekine, M.; Hata, T. *J. Chem. Soc., Perkin Trans. 1* **1976**, 1711−1716.
(21) Walt, D. R.; Findeis, M. A.; Rios-Mercadillo, V. M.; Augé, J.; Whitesides, G. M. *J. Am. Chem. Soc.* **1984**, *106*, 234−239.
(22) Shimazu, M.; Shinozuka, K.; Sawai, H. *Tetrahedron Lett.* **1990**, *31*, 235−238.
(23) Lee, J.; Churchil, H.; Choi, W.-B.; Lynch, J. E.; Roberts, F. E.; Volante, R. P.; Reider, P. J. *Chem. Commun.* **1999**, 729−730.
(24) Dowden, J.; Moreau, C.; Brown, R. S.; Berridge, G.; Galione, A.; Potter, B. V. L *Angew. Chem., Int. Ed.* **2004**, *43*, 4637−4640.
(25) Jin, L.; Wei, W.; Jiang, Y.; Peng, H.; Cai, J.; Mao, C.; Dai, H.; Choy, W.; Bemis, J. E.; Jirousek, M. R.; Milne, J. C.; Westphal, C. H.; Perni, R. B. *J. Biol. Chem.* **2009**, *284*, 24394−24405.
(26) Du, J.; Zhou, Y.; Su, X.; Yu, J. J.; Khan, S.; Jiang, H.; Kim, J.; Woo, J.; Kim, J. H.; Choi, B. H.; He, B.; Chen, W.; Zhang, S.; Cerione, R. A.; Auwerx, J.; Hao, Q.; Lin, H. *Science* **2011**, *334*, 806−809.
(27) Vince, R.; Daluge, S. *J. Org. Chem.* **1980**, *45*, 531−533.
(28) Tadano, K.-i.; Hoshino, M.; Ogawa, S.; Suami, T. *J. Org. Chem.* **1988**, *53*, 1427−1432.
(29) Tadano, K.-i.; Hoshino, M.; Ogawa, S.; Suami, T. *Tetrahedron Lett.* **1987**, *28*, 2741−2744.
(30) Shealy, Y. F.; Clayton, J. D. *J. Am. Chem. Soc.* **1969**, *91*, 3075−3083.
(31) Shealy, Y. F.; Clayton, J. D. *J. Am. Chem. Soc.* **1966**, *88*, 3885−3887.
(32) Rassu, G.; Auzzas, L.; Pinna, L.; Zambrano, V.; Zanardi, F.; Battistini, L.; Marzocchi, L.; Acquotti, D.; Casiraghi, G. *J. Org. Chem.* **2002**, *2002*, 5338−5342.
(33) Rassu, G.; Auzzas, L.; Pinna, L.; Battistini, L.; Zanardi, F.; Marzocchi, L.; Acquotti, D.; Casiraghi, G. *J. Org. Chem.* **2000**, *65*, 6307−6318.
(34) Paulsen, H.; Maaß, U. *Chem. Ber.* **1981**, *114*, 346−358.
(35) Parry, R. J.; Haridas, K.; De Jong, R.; Johnson, C. R. *J. Chem. Soc., Chem. Commun.* **1991**, 740−741.
(36) Mikhailopulo, I. A.; Pricota, T. I.; Timoshchuk, V. A.; Akhrem, A. A. *Synthesis* **1980**, 388−389.
(37) Madhavan, G. V. B.; Martin, J. C. *J. Org. Chem.* **1986**, *51*, 1287−1293.
(38) Lehrman, T. E.; Greenberg, W. A.; Liberles, D. A.; Wada, C. K.; Dervan, P. B. *Helv. Chim. Acta* **1997**, *80*, 2002−2022.
(39) LeGrand, D. M.; Roberts, S. M. *J. Chem. Soc., Perkin Trans. 1* **1992**, 1751−1752.

(40) Katagiri, N.; Muto, M.; Nomura, M.; Higashikawa, T.; Kaneko, C. *Chem. Pharm. Bull.* **1991**, *39*, 1112−1122.
(41) Kam, B. L.; Oppenheimer, N. J. *J. Org. Chem.* **1981**, *46*, 3268−3272.
(42) Ikbal, M.; Cerceau, C.; Le Goffic, F.; Sicsic, S. *Eur. J. Med. Chem.* **1989**, *24*, 415−420.
(43) Hronowski, L. J. J.; Szarek, W. A. *Can. J. Chem.* **1986**, *64*, 1620−1629.
(44) Cermak, R. C.; Vince, R. *Tetrahedron Lett.* **1981**, *22*, 2331−2332.
(45) Boyer, S. J.; Leahy, J. W. *J. Org. Chem.* **1997**, *62*, 3976−3980.
(46) Arita, M.; Adachi, K.; Ito, Y.; Sawai, H.; Ohno, M. *J. Am. Chem. Soc.* **1983**, *105*, 4049−4055.
(47) Griffiths, G. J.; Previdoli, F. E. *J. Org. Chem.* **1993**, *58*, 6129−6131.
(48) Taylor, S. J. C.; Brown, R. C.; Keene, P. A.; Taylor, I. N. *Bioorg. Med. Chem.* **1999**, *7*, 2163−2168.
(49) Brown, H. C.; Hébert, N. C. *J. Organomet. Chem.* **1983**, *255*, 135−141.
(50) Marvell, E. N.; Shahidi, I. *J. Am. Chem. Soc.* **1970**, *92*, 5646−5649.
(51) Schwer, B.; Bunkenborg, J.; Verdin, R. O.; Andersen, J. S.; Verdin, E. *Proc. Natl. Acad. Sci. U.S.A.* **2006**, *103*, 10224−10229.
(52) Nakagawa, T.; Lomb, D. J.; Haigis, M. C.; Guarente, L. *Cell* **2009**, *137*, 560−570.
(53) Peng, C.; Lu, Z.; Xie, Z.; Cheng, Z.; Chen, Y.; Tan, M.; Luo, H.; Zhang, Y.; He, W.; Yang, K.; Zwaans, B. M.; Tishkoff, D.; Ho, L.; Lombard, D.; He, T. C.; Dai, J.; Verdin, E.; Ye, Y.; Zhao, Y. *Mol. Cell. Proteomics* **2011**, *10*, M111.012658.
(54) Altamore, T. M.; Duggan, P. J.; Krippner, G. Y. *Bioorg. Med. Chem.* **2006**, *14*, 1126−1133.
(55) Tsukamoto, H.; Kahne, D. *Bioorg. Med. Chem. Lett.* **2011**, *21*, 5050−5053.
(56) Abraham, R. J.; Koniotou, R.; Sancassan, F. *J. Chem. Soc., Perkin Trans. 2* **2002**, 2025−2030.
(57) Moinuddin, S. G. A.; Youn, B.; Bedgar, D. L.; Costa, M. A.; Helms, G. L.; Kang, C.; Davin, L. B.; Lewis, N. G. *Org. Biomol. Chem.* **2006**, *4*, 808−816.
(58) Otwinowski, Z.; Minor, W. *Methods Enzymol.* **1997**, *276*, 307−326.
(59) Leslie, A. G. W. *Joint CCP4 and ESF-EACBM Newsletter on Protein Crystallography* **1992**, *27*, 30.
(60) Evans, P. *Acta Crystallogr., Sect. D: Biol. Crystallogr.* **2006**, *62*, 72−82.
(61) Murshudov, G. N.; Vagin, A. A.; Dodson, E. J. *Acta Crystallogr., Sect. D: Biol. Crystallogr.* **1997**, *53*, 240−255.
(62) Bailey, S. *Acta Crystallogr., Sect. D: Biol. Crystallogr.* **1994**, *50*, 760−763.
(63) McCoy, A. J.; Grosse-Kunstleve, R. W.; Adams, P. D.; Winn, M. D.; Storoni, L. C.; Read, R. J. *J. Appl. Crystallogr.* **2007**, *40*, 658−674.
(64) Adams, P. D.; Grosse-Kunstleve, R. W.; Hung, L. W.; Ioerger, T. R.; McCoy, A. J.; Moriarty, N. W.; Read, R. J.; Sacchettini, J. C.; Sauter, N. K.; Terwilliger, T. C. *Acta Crystallogr., Sect. D: Biol. Crystallogr.* **2002**, *58*, 1948−1954.
(65) Emsley, P.; Cowtan, K. *Acta Crystallogr., Sect. D: Biol. Crystallogr.* **2004**, *60*, 2126−2132.